



**HAL**  
open science

# Synthesis of Polyethylene Vitrimers in a Single Step: Consequences of Graft Structure, Reactive Extrusion Conditions, and Processing Aids

Mohamad Maaz, Alexi Riba-Bremerch, Clément Guibert, Nathan van Zee,  
Renaud Nicolaÿ

► **To cite this version:**

Mohamad Maaz, Alexi Riba-Bremerch, Clément Guibert, Nathan van Zee, Renaud Nicolaÿ. Synthesis of Polyethylene Vitrimers in a Single Step: Consequences of Graft Structure, Reactive Extrusion Conditions, and Processing Aids. *Macromolecules*, 2021, 54 (5), pp.2213-2225. 10.1021/acs.macromol.0c02649 . hal-03376321

**HAL Id: hal-03376321**

**<https://hal.science/hal-03376321>**

Submitted on 1 Dec 2021

**HAL** is a multi-disciplinary open access archive for the deposit and dissemination of scientific research documents, whether they are published or not. The documents may come from teaching and research institutions in France or abroad, or from public or private research centers.

L'archive ouverte pluridisciplinaire **HAL**, est destinée au dépôt et à la diffusion de documents scientifiques de niveau recherche, publiés ou non, émanant des établissements d'enseignement et de recherche français ou étrangers, des laboratoires publics ou privés.

# Synthesis of Polyethylene Vitrimers in a Single Step: Consequences of Graft Structure, Reactive Extrusion Conditions, and Processing Aids

*Mohamad Maaz,<sup>1</sup> Alexi Riba-Bremerch,<sup>1</sup> Clément Guibert,<sup>2</sup> Nathan J. Van Zee,<sup>1\*</sup> Renaud Nicolay<sup>1\*</sup>*

<sup>1</sup>Chimie Moléculaire, Macromoléculaire, Matériaux, ESPCI Paris, Université PSL, CNRS, 75005 Paris, France.

<sup>2</sup>Sorbonne Université, CNRS, Laboratoire de Réactivité de Surface, F-75005 Paris, France.

**KEYWORDS:** vitrimers, reactive extrusion, processing, grafting, dioxaborolane metathesis.

**ABSTRACT:** Vitrimers have captured broad interest in academia and industry because they offer a compelling combination of mechanical performance, thermal stability, and recyclability. They are permanent polymer networks that contain dynamic covalent bonds that undergo thermally-activated exchange reactions without decreasing the connectivity of the network. The introduction of such functionality to commercial thermoplastics via reactive processing is envisioned to be an economical way to access high-performance, recyclable materials. Polyolefins are of particular interest because they are the most widely used class of polymers today. Although reactive processing is widely practiced in industry, it remains a nascent approach for accessing polyolefin vitrimers. Herein, we report a dimaleimide bis(dioxaborolane) that allows for commercial polyethylene (PE) to be transformed into a

vitriimer in a single step without any small molecule byproducts. The miscibility of the grafting agent with the PE melt is a critical consideration for optimizing the grafting protocol, as efficient mixing is essential for achieving quantitative grafting and a high gel content. We find that the degree of incompatibility of the grafting agent in the PE melt strongly affects the nano- and macrostructure of the resulting PE vitrimers, which in turn dictates the thermal and mechanical properties. Finally, the material properties can be finely tuned using a reactive processing aid.

## **Introduction**

Vitrimers are permanent polymer networks that have captured the interest of both academia and industry because they offer a compelling combination of mechanical performance, thermal stability, and recyclability. These properties are derived from thermally-activated exchange reactions that take place between dynamic covalent crosslinks without decreasing the connectivity of the network. A consequence of this design is that the viscoelastic properties of the material are strongly influenced by the kinetics of the exchange reaction. At service temperature, the rate of exchange is slow, which suppresses shuffling of the connectivity of the network and causes the material to behave like a typical thermoset. At processing temperatures, the exchange rate is fast, causing the network connectivity to rearrange and the material to flow like an amorphous glass. A wide variety of dynamic covalent crosslinks have been implemented into many different kinds of polymer matrices as comprehensively reviewed elsewhere.<sup>1-7</sup>

There are numerous strategies for introducing dynamic covalent bonds into a polymer matrix to create a vitriimer. For instance, conventional epoxy-acid and epoxy-anhydride resins can be converted into vitrimers simply by adding a transesterification catalyst.<sup>8-10</sup> In this case, the dynamic covalent bonds (i.e., the ester bonds) are already present in the polymer network. The addition of a catalyst decreases the activation energy of exchange between the ester groups

and the free alcohol groups, permitting dynamic transesterification reactions to proceed within a practically useful temperature range.

For other kinds of polymers, such as those with backbones that are purely constituted of carbon-carbon single bonds, dynamic covalent bonds (or a precursor to such functionalities) must be explicitly introduced either in the synthesis of the polymer or through post-polymerization modification. An important example is polyethylene (PE) because it is the most widely produced and consumed polymer today.<sup>11</sup> Converting PE into a vitrimer is an appealing way to enhance its melt strength, creep resistance, environmental stress cracking resistance, and recyclability while retaining its desirable processing properties. Several PE-based vitrimers have been reported with different kinds of dynamic exchange chemistries, including dioxaborolane metathesis,<sup>12-15</sup> transesterification,<sup>16</sup> silyl ether exchange,<sup>17</sup> and vinylogous urethane exchange.<sup>18</sup>

Our laboratory is particularly interested in using reactive extrusion to introduce dioxaborolane-based dynamic crosslinks into PE. Reactive grafting is an appealing industrial process that does not require solvents or purification.<sup>19-20</sup> Dioxaborolane groups undergo catalyst-free metathesis reactions via an associative mechanism (Figure 1), and they feature high thermal stability and convenient chemical orthogonality.<sup>12,21-22</sup> This approach was first realized by exploiting the radical-initiated grafting of maleimides in a two-step reactive extrusion protocol.<sup>12</sup> In short, high-density PE is reacted with the maleimide dioxaborolane **A** in the presence of dicumyl peroxide in a twin-screw micro-compounder to obtain a dioxaborolane-grafted PE (Figure 2, top). Before extruding this material, bis(dioxaborolane) **C** is added to crosslink the material via exchange reactions; the small molecule **D** is liberated into the matrix as a byproduct. The resulting material **V-AC** exhibits a storage modulus above the melting temperature ( $T_m$ ) and enhanced creep resistance compared to that of virgin PE, which are both consistent with the formation of a vitrimer.

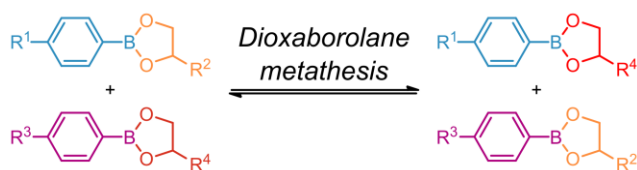


**Figure 1.** Dioxaborolane metathesis.

Subsequent studies have revealed that **V-AC** exhibits complex meso- and nanostructures that have important consequences on how the vitrimer flows.<sup>13,15</sup> The incompatibility between the PE matrix and the dioxaborolane units cause the material to form a hierarchical structure. The PE vitrimer is essentially a phase-separated blend of two distinct macrophases: an insoluble, crosslink-rich phase and a soluble, crosslink-poor phase. On the basis of small angle X-ray scattering (SAXS), the insoluble phase contains aggregates of dioxaborolane grafts that assemble into a fractal structure; these features are also evident in the blends of the insoluble and soluble phases.<sup>13</sup> Rheological studies reveal that the soluble phase serves as a lubricant and binding agent, allowing the vitrimer to easily flow via a melt fracture-healing mechanism when subjected to high stress.<sup>15</sup>

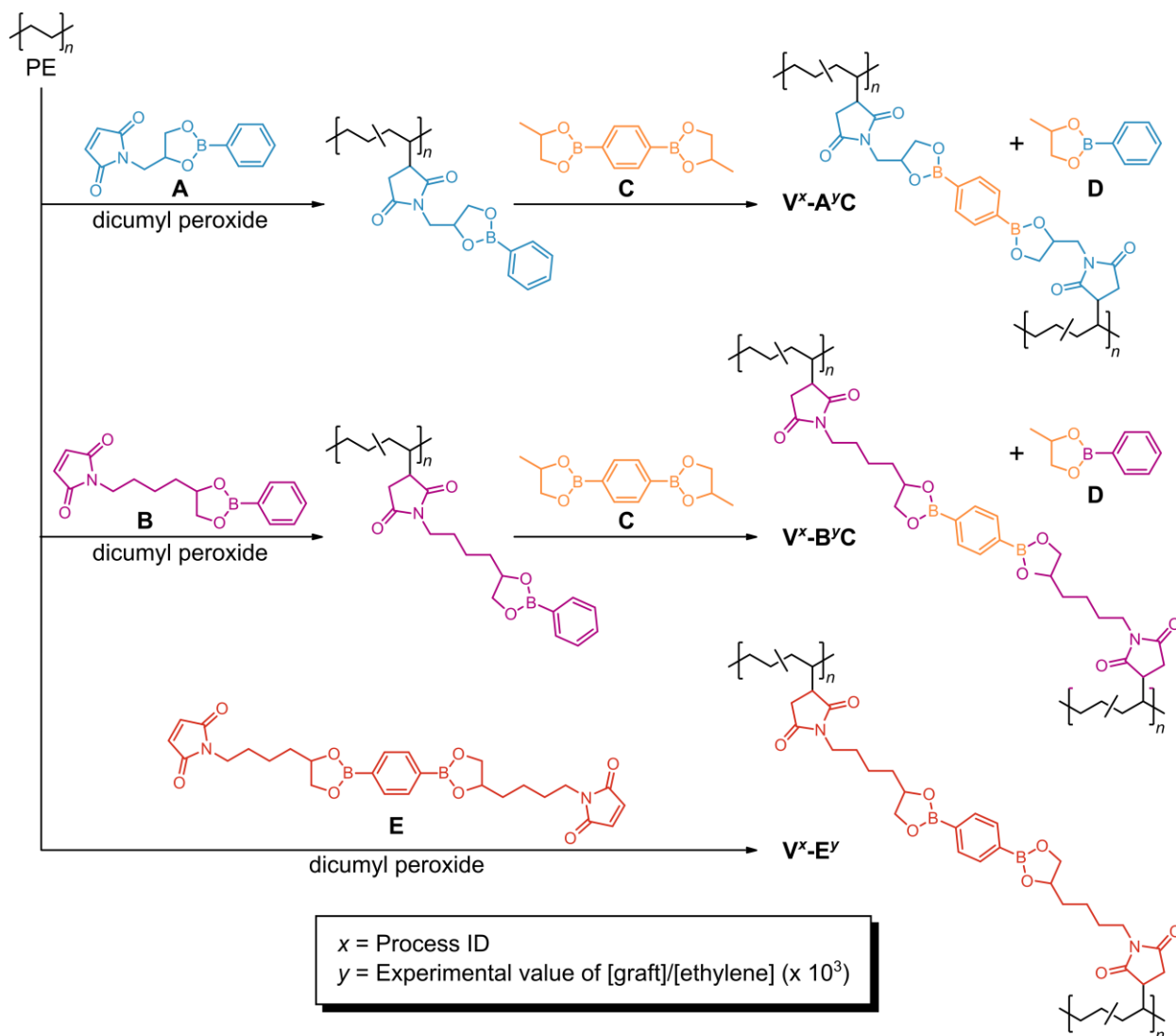


**Figure 2.** Synthesis of PE vitrimers using grafting agents **A** (with **C**), **B** (with **C**), and **E**.

A major disadvantage associated with the use of **A** and **C** for making PE vitrimers, however, is the release of **D** because it can leach from the material over time. It is possible to remove **D** by an additional washing step,<sup>13,15</sup> but this is not a scalable process. Our group has previously exemplified a single-step functionalization of PE by reactive extrusion using dinitroxide bis(dioxaborolane) crosslinkers.<sup>14</sup> Although small molecules are not released in the course of crosslinking, the grafted crosslinking unit suffers from poor thermal stability at conventional processing temperatures. Other reports that describe the synthesis of PE vitrimers entail the

incorporation of functional groups at the stage of PE synthesis,<sup>16-18,23-24</sup> which is not ideal for recycling applications.

Herein, we describe the synthesis and utilization of a dimaleimide bis(dioxaborolane) grafting agent that allows for commercial PE to be transformed into a vitrimer in a single step by reactive extrusion. We optimized the processing conditions to allow for quantitative grafting, and we characterized the resulting vitrimers by a comprehensive battery of spectroscopic, calorimetric, microscopic, X-ray scattering, and mechanical testing techniques. The homogeneity of the grafting in the soluble and insoluble fractions is found to be directly related to the immiscibility of the grafting agent in the polyethylene melt. Thus, even small changes to the structure of the grafting agent and the processing parameters give rise to profound consequences on the structure and physical properties of the resulting PE vitrimers.

## Experimental Section

**Materials.** Maleimide (99%), furan (99%), 1,2,6-hexanetriol (96%), *p*-toluenesulfonic acid monohydrate (98%), methanesulfonyl chloride (99%), trimethylamine (98%), 3-amino-1,2-propanediol (97%), and dicumyl peroxide (DCP, 98%) were purchased from Sigma Aldrich. Maleic anhydride (99%), 1,2-octanediol (93%), phenylboronic acid (97%) and benzene-1,4-diboronic acid (98%) were purchased from TCI Chemicals. Solvents were purchased from Carlo Erba. All reagents were used without further purification. High-density polyethylene (PE, melt flow index 2.49 g/10min at 190°C with 5 kg weight) was provided by Aliaxis R&D. By high temperature size exclusion chromatography (vide infra), this polymer has a number average molar mass of 35.4 kDa and a dispersity of 2.76.

The maleimide dioxaborolanes 1-((2-phenyl-1,3,2-dioxaborolan-4-yl)methyl)-1H-pyrrole-2,5-dione (**A**) and 1,4-bis(4-methyl-1,3,2-dioxaborolan-2-yl)benzene (**C**) were synthesized according to previously-reported procedures.<sup>12</sup> The synthesis of 1-(4-(2-phenyl-1,3,2-

dioxaborolan-4-yl)butyl)-1H-pyrrole-2,5-dione (**B**), 1,1'-((1,4-phenylenebis(1,3,2-dioxaborolane-2,4-diyl))bis(butane-4,1-diyl))bis(1H-pyrrole-2,5-dione) (**E**), 4-decyl-2-phenyl-1,3,2-dioxaborolane (**F**), and 1,1'-((1,4-phenylenebis(1,3,2-dioxaborolane-2,4-diyl))bis(methylene))bis(1H-pyrrole-2,5-dione) (**G**) are detailed in the Supporting Information (SI).

**Nuclear Magnetic Resonance (NMR) Spectroscopy.**  $^1\text{H}$  and  $^{13}\text{C}$  NMR spectra were recorded at 24 °C using a Bruker AVANCE 400 spectrometer at 400 and 100 MHz, respectively. Spectra were referenced to the residual solvent peaks. For  $^1\text{H}$  NMR:  $\delta$  7.26 in  $\text{CDCl}_3$  and  $\delta$  2.50 in  $(\text{CD}_3)_2\text{SO}$ . For  $^{13}\text{C}$  NMR:  $\delta$  77.16 in  $\text{CDCl}_3$  and  $\delta$  39.50 in  $(\text{CD}_3)_2\text{SO}$ . Raw spectra are presented in Figures S29–S47 (SI).

**High Temperature Size Exclusion Chromatography (HT-SEC).** The molar mass of the virgin PE was determined by HT-SEC at the laboratory of Chemistry, Catalysis, Polymers, and Process (C2P2) at the University of Lyon. This measurement was performed at 150 °C in 1,2,4-trichlorobenzene (stabilized by 0.2 g L<sup>-1</sup> of butylated hydroxytoluene) on a Malvern Panalytical Viscotek SEC instrument equipped with a triple-detection unit and three separation columns from Polymer Standard Services (POLEFIN 300 mm × 8 mm; i.d. porosity of 103, 105, and 106 Å). Molar masses were calculated using conventional calibration with linear polyethylene standards.

**Grafting of Dioxaborolane Maleimides via Reactive Extrusion.** All PE vitrimers were prepared by reactive extrusion using a DSM Xplore batch twin-screw micro-compounder with a 5 cm<sup>3</sup> capacity. The system has a co-rotating conical screw profile and a recirculation channel that permits control over the residence time. Grafting was performed with a screw speed of 100 rpm under a flow of nitrogen. Five different reactive extrusion protocols were used:

**Protocol P1a:** This protocol is a close adaptation of the one reported by Röttger et al.<sup>12</sup> A dry blend of PE, either **A** or **B**, and DCP (1.5 mg, 0.05 wt%) is loaded into the micro-

compounder over approximately 2 min with the barrel temperature set at 170 °C. After a subsequent residence time of 8 min, 0.5 molar equivalents (with respect to the molar loading of **A** or **B**) of **C** is rapidly added. After an additional 6 min residence time, the contents are extruded.

**Protocol P1b:** A dry blend of PE, **E**, and DCP (1.5 mg, 0.05 wt%) is loaded into the micro-compounder over approximately 2 min with the barrel temperature set at 170 °C. After a subsequent residence time of 8 min, the contents are extruded.

**Protocol P2a:** A dry blend of PE and either **A** or **B** is loaded into the micro-compounder over approximately 2 min with the barrel temperature set at 140 °C. After a subsequent residence time of 2 min, the temperature of the barrel is increased to 170 °C; the temperature ramp requires about 1 min. Just as the barrel reaches 170 °C, DCP (1.5 mg, 0.05 wt%) that is loaded on a small disc of PE (approximately 25 mg) is rapidly added. After a residence time of 8 min, 0.5 molar equivalents (with respect to the molar loading of **A** or **B**) of **C** is rapidly added. After an additional 6 min residence time, the contents are extruded.

**Protocol P2b:** A dry blend of PE and **E** is loaded into the micro-compounder over approximately 2 min with the barrel temperature set at 140 °C. After a subsequent residence time of 2 min, the temperature of the barrel is increased to 170 °C; the temperature ramp requires about 1 min. Just as the barrel reaches 170 °C, DCP (1.5 mg, 0.05 wt%) that is loaded on a small disc of PE (approximately 25 mg) is rapidly added. After a residence time of 8 min, the contents are extruded.

**Protocol P2c.** This process is the same as protocol **P2b**, except with the following addition: after the addition of DCP and the subsequent 8 min of residence time, compound **F** is added, and mixing is continued for an additional 6 minutes before the contents are extruded.

**Diolysis.** A given sample (200 mg) was heated overnight in xylene (40 mL with 0.5 wt% BHT) at 130 °C with an excess 1,2-octanediol (approximately 100 molar equivalents with

respect to the dioxaborolane units) to cleave the dioxaborolane crosslinks and solubilize the polymer, which was then isolated by precipitating in acetone, filtering, and drying at 150 °C under vacuum for several hours.

**Quantification of Grafting Yields.** Grafting was quantified by Fourier transform infrared (FTIR) spectroscopy using a Bruker Tensor 37 spectrometer. To determine the extinction coefficients for each diagnostic band, calibration curves were prepared using chloroform solutions of different concentrations of **A**, **E**, **F**, and docosane (i.e., an oligomeric analogue of PE). Measurements were carried out using a liquid cell with KCl windows. The area under each diagnostic band linearly scaled with solute molar concentration (Figures S1, SI), and the extinction coefficients for each band were calculated using the Beer-Lambert law (Figures S2, SI).

The diagnostic bands for each small molecule in solution matched the corresponding signals observed in the spectra of the vitrimers. The maleimide dioxaborolane **A** and the resulting succinimide moiety of **A**-based grafts exhibit a C=O stretching band at 1710 cm<sup>-1</sup> ( $\epsilon_{1710,A} = 2.67 \pm 0.05 \text{ M}^{-1} \cdot \mu\text{m}^{-1}$ ), which agrees with the literature value.<sup>13</sup> The dimaleimide bis(dioxaborolane) **E** and the resulting succinimide moiety of **E**- and **B**-based grafts also exhibit a C=O stretching band at 1710 cm<sup>-1</sup> but with a different extinction coefficient ( $\epsilon_{1710,E} = 2.91 \pm 0.08 \text{ M}^{-1} \cdot \mu\text{m}^{-1}$ ). The 1,4-bis(dioxaborolanyl)benzene units exhibit a C=C stretching band at 1520 cm<sup>-1</sup> ( $\epsilon_{1520,E} = 0.34 \pm 0.01 \text{ M}^{-1} \cdot \mu\text{m}^{-1}$ ), and the phenyl dioxaborolane units exhibit a C=C stretching band at 1600 cm<sup>-1</sup> ( $\epsilon_{1600,F} = 0.14 \pm 0.01 \text{ M}^{-1} \cdot \mu\text{m}^{-1}$ ). The CH<sub>2</sub> scissoring band attributable to the PE backbone is at 1470 cm<sup>-1</sup> ( $\epsilon_{1470,\text{docosane}} = 0.043 \pm 0.001 \text{ M}^{-1} \cdot \mu\text{m}^{-1}$ , calculated on the basis of moles of C<sub>2</sub>H<sub>4</sub> units).

For the vitrimer samples, absorbance spectra were recorded using a Specac Goldengate attenuated total reflection (ATR) cell. The dependence of the IR wave penetration depth on the wavenumber was corrected within the acquisition software (Bruker OPUS). The molar ratios

of [graft]/[ethylene], [crosslink]/[graft], and [phenyl]/[graft] were thus calculated using the Beer-Lambert law as follows in eqs 1–4:

$$\frac{C_{\text{graft}}}{C_{\text{ethylene}}} = \frac{A_{1710}}{A_{1470}} \cdot \frac{\varepsilon_{1470}}{\varepsilon_{1710}} \quad (1)$$

$$\frac{C_{\text{crosslink}}}{C_{\text{graft}}} = \frac{A_{1520}}{A_{1710}} \cdot \frac{\varepsilon_{1710}}{\varepsilon_{1520}} \quad (2)$$

$$\frac{C_{\text{phenyl}}}{C_{\text{ethylene}}} = \frac{A_{1600}}{A_{1470}} \cdot \frac{\varepsilon_{1470}}{\varepsilon_{1600}} \quad (3)$$

$$\frac{C_{\text{phenyl}}}{C_{\text{graft}}} = \frac{C_{\text{phenyl}}}{C_{\text{ethylene}}} \cdot \frac{C_{\text{ethylene}}}{C_{\text{graft}}} \quad (4)$$

where  $A_i$  is the area of the peak at wavenumber  $i$ ,  $\varepsilon_j$  is the absorption coefficient of the peak at wavenumber  $j$ , and  $C_{\text{phenyl}}$  is the concentration of phenyl dioxaborolane group attributable to unreacted **A**-based grafts, unreacted **B**-based grafts, **D**, and **F** in the PE matrix (as specified in the text).

**Separation of Soluble and Insoluble Fractions.** In a typical experiment, approximately 200 mg of sample ( $m_0$ ) is wrapped with a woven stainless wire mesh cage and heated overnight in 40 mL xylene (0.5 wt% BHT) at 130 °C. The cage is then removed, washed with acetone, and then dried under vacuum at 150 °C for several hours. The mass of the insoluble fraction trapped in the cage is measured ( $m_f$ ), and the gel content was determined using the following formula:  $m_f / m_0 \times 100$ . The soluble fraction was recovered by precipitation in acetone and filtration, followed by drying in a vacuum oven at 150 °C.

**Melt Flow Index (MFI) Determination.** The MFI was determined at 190 °C using either a 5.0 or 21.6 kg load (specified in the tabulated data) according to ISO 1133 using a Zwick plastometer (Zwick GmbH, Ulm, Germany). In short, after a 5 min pre-heating period, 10 sections were collected at time intervals adapted to each sample flow rate. The MFI results were converted into amounts of flown material per 10 min.

**Differential Scanning Calorimetry (DSC).** For each sample, approximately 5–10 mg of material was loaded into a hermetically-sealed, disposable aluminum pan. DSC experiments

were performed on a TA Instruments Discovery 250 DSC that was equipped with an autosampler and a liquid nitrogen cooling system. The following temperature program was used for vitrimer samples: 50 to 200 °C at +10 °C·min<sup>-1</sup>; then 200 to 50 °C at -10 °C·min<sup>-1</sup>; then 50 to 200 °C at +10 °C·min<sup>-1</sup>. The reported melting temperature ( $T_m$ ) and enthalpy of melting ( $\Delta H_m$ ) for each vitrimer were determined on the basis of the second heating cycle. The degree of crystallinity ( $\chi_c$ ) was calculated using the equation  $\chi_c = \Delta H_m \cdot (\Delta H_m^+)^{-1}$ , where  $\Delta H_m^+$  is the specific enthalpy of melting of a fully crystalline polyethylene and is reported to be 293 J·g<sup>-1</sup>.<sup>25</sup> Reported values are the average of two measurements.

**Thermogravimetric Analysis (TGA).** For each sample, approximately between 10 and 15 mg of material was loaded into disposable aluminum pans. A Netzsch TG 209 F1 Libra was used with a nitrogen atmosphere. The temperature program consisted of heating from 25 to 600 °C at 10 °C·min<sup>-1</sup>.

**Dynamic Mechanical Analysis (DMA).** Samples for DMA were shaped into rectangular bars (1.4 mm × 5 mm × 35 mm) by compression molding at 150 °C for 10 minutes. A TA Instruments Q800 analyzer was used in tension mode with a heating rate of 3 °C·min<sup>-1</sup> from 30 to 260 °C, a maximum strain amplitude of 1%, and a fixed frequency of 1 Hz.

**Tensile Testing.** Dogbone-shaped samples (ISO 527-2 type 5B) were prepared by compression molding at 150 °C for 10 min. Tensile stress-strain experiments were conducted on an Instron universal testing system. The crosshead speed was set to 10 mm·min<sup>-1</sup>. Five specimens of each sample were tested for reproducibility. Young's modulus was calculated from the slope of the line between strain values of 0.05 and 0.25 %.

**Stress Relaxation Experiments.** Disc-shaped samples (25 mm diameter, 1.4 mm thickness) were prepared by compression molding. Stress relaxation experiments were performed on an Anton Paar MCR 501 rotational rheometer with a parallel plate geometry (25 mm diameter) in a convection oven under a nitrogen atmosphere. Measurements were conducted by applying a

constant shear strain of 1%. A normal force of 0.1 N was maintained throughout the measurement to ensure contact with the sample. When full relaxation is achieved, the zero-shear viscosity  $\eta_0$  and the relaxation time  $\tau$  were calculated from stress relaxation experiments using equations 5 and 6:

$$\eta_0 = \int_0^{\infty} G(t)dt \quad (5)$$

$$\tau = \frac{\int_0^{\infty} t G(t)dt}{\int_0^{\infty} G(t)dt} \quad (6)$$

**Polarized Optical Microscopy (POM).** Thin film samples of approximately 150  $\mu\text{m}$  were prepared by compression molding and observed between a microscopic slide and a cover glass. Micrographs were taken between crossed polarizers using a digital camera (Sony XCD-U100CR) attached to an optical microscope (Leica DMRXE) that was equipped with a hot stage (Linkam LTS350). Cooling and heating rates used for dynamic experiments were  $-5$  and  $+5$   $^{\circ}\text{C}\cdot\text{min}^{-1}$ , respectively. The temperature program was: first heating to  $100$   $^{\circ}\text{C}$ , then a picture is recorded every degree during the heating step from  $100$   $^{\circ}\text{C}$  to  $170$   $^{\circ}\text{C}$  and during the cooling step from  $170$   $^{\circ}\text{C}$  to  $90$   $^{\circ}\text{C}$ . Before the cooling step, samples were held at  $170$   $^{\circ}\text{C}$  for 2 min to erase their thermal history. The melting ( $T_m$ ) and crystallization temperatures ( $T_c$ ) of the PE vitrimers were taken to be the disappearance and reappearance of birefringent crystalline structures, respectively, at  $100\times$  magnification.

**Powder X-ray Diffraction (XRD).** Wide-angle X-ray scattering (WAXS) patterns were recorded in transmission with a multi-angle detector. The wavelength used was Cu  $K_{\alpha}$  ( $\lambda = 1.54$   $\text{\AA}$ ) from an X-ray generator (Phillips X-Pert) operating at 40 kV and 40 mA. The spectra were recorded in the  $2\theta$  range of  $5-38^{\circ}$  (step size  $0.033^{\circ}$  and time 99.7 s) with fixed divergence slits ( $1/4^{\circ}$  and  $1/2^{\circ}$ ) and an incident beam mask of 15 mm. Experiments were performed at room temperature on compression molded samples (10 minutes at  $150$   $^{\circ}\text{C}$  and then slowly cooled to room temperature while in the mold) with a thickness of 1.4 mm. WAXS patterns

were analyzed using Origin. The distance between atomic layers in the PE crystals (*d*-spacing) was calculated using Bragg's law:

$$d_{hkl} = \frac{\lambda}{2\sin\theta_{hkl}} \quad (7)$$

in which  $d_{hkl}$  is the *d*-spacing,  $\lambda$  is the Cu K $\alpha$  radiation wavelength, and  $2\theta_{hkl}$  is the scattering angle. The degree of crystallinity  $\chi_c$  (WAXS) of samples was calculated using the equation:<sup>26</sup>

$$\chi_c(WAXS) = \frac{A_c}{(A_c + A_a)} \times 100\% \quad (8)$$

in which  $A_c$  and  $A_a$  are the areas under fitted crystalline and amorphous halo, respectively. The crystallite size normal to the given *hkl* plane ( $D_{hkl}$ ) was estimated using the Scherrer formula:<sup>27-</sup>

28

$$D_{hkl} = \frac{0,9\lambda}{\Delta(2\theta_{hkl})\cos\theta_{hkl}} \quad (9)$$

where  $\lambda$  is the Cu K $\alpha$  radiation wavelength,  $2\theta$  is the scattering angle, and  $\Delta(2\theta_{hkl})$  is the peak width at the half-maximum (FWHM).

**Small-Angle X-ray Scattering (SAXS).** Samples for SAXS were shaped into bars (1.4 mm  $\times$  5 mm  $\times$  35 mm) by compression molding at 150 °C for 10 minutes and then slowly cooled to room temperature in the mold. Small-angle X-ray scattering measurements were conducted at the SWING beamline at the SOLEIL Synchrotron Source (Saint-Aubin, FR). They were performed at a wavelength  $\lambda = 1.03 \text{ \AA}$  ( $E = 12 \text{ keV}$ ) and recorded through a detector localized at a distance of 4 m from the sample to cover the scattering vector ( $q$ ) range of 0.0018–0.28  $\text{\AA}^{-1}$ . No subtraction was applied to the diffractograms, as they were not sealed between windows. The software Foxtrot was used to process the data reduction from 2D images to 1D diffractograms. Electron density correlation functions were computed through the SasView software.<sup>29</sup>

**Calculation of Average Crosslinking Density.** Consider an E-based vitrimer that contains  $x$  grafts per  $10^3$  ethylene units,  $x/2$  equivalents of 1,4-bis(dioxaborolanyl)benzene crosslinking

unit, and  $y$  units of **F** per  $10^3$  ethylene units. Assuming equal reactivity among all dioxaborolane groups, the following equations define the probability for a crosslinking unit to be bonded to a polymer chain on both sides ( $p_{\text{crosslinked}}$ ), to be bonded on one side to a polymer chain and on the other side to a 1,2-dodecanediol unit derived from **F** ( $p_{\text{pendant}}$ ), and to be bonded on both sides to 1,2-dodecanediol units derived from **F** ( $p_{\text{free}}$ ):

$$p_{\text{crosslink}} = \left(\frac{x}{x+y}\right)^2 \quad (10)$$

$$p_{\text{pendant}} = \frac{2xy}{(x+y)^2} \quad (11)$$

$$p_{\text{free}} = \left(\frac{y}{x+y}\right)^2 \quad (12)$$

The average crosslinking density ( $D_{\text{crosslink}}$ ) per  $10^3$  ethylene units is thus calculated as follows:

$$D_{\text{crosslink}} = \frac{x}{2} p_{\text{crosslink}} \quad (13)$$

## Results and Discussion

### Design, Synthesis, and Thermal Stability of New Dioxaborolane-Based Crosslinkers.

We envisioned that PE vitrimers could be accessed in a single step and without the formation of a small molecule byproduct by using a dimaleimide bis(dioxaborolane) unit. A key practical consideration is that the  $T_m$  of the grafting agent should be below the temperature at which the reactive extrusion is performed to facilitate mixing in the PE melt. In this study, grafting reactions were carried out in a  $5 \text{ cm}^3$  twin-screw micro-compounder at  $170 \text{ }^\circ\text{C}$  with a residence time of 8 min, which corresponds to six-times the half-life of dicumyl peroxide (DCP) at this temperature.

Initially, a dimaleimide bis(dioxaborolane) analogue of **A** ( $T_m = 93 \text{ }^\circ\text{C}$ ) with a benzene-1,4-bis(dioxaborolane) core was targeted. This compound (**G**, **SI**) was synthesized, but it was found to have a melting transition that is too high for reactive extrusion under our targeted conditions ( $T_m = 215 \text{ }^\circ\text{C}$ ). We anticipated that the  $T_m$  could be adjusted by changing the length of the

spacer between the maleimide and dioxaborolane functional groups. An analogue of **A** that contains a butyl spacer, **B** (Figure 2), exhibits a  $T_m$  (122 °C) that is higher than that of **A**. Gratifyingly, the bis(maleimide dioxaborolane) analogue **E** exhibits a  $T_m$  of 158 °C, which is below our desired processing temperature. Compounds **B** and **E** were thus synthesized on multi-gram scale in 44 and 41% yields, respectively, over 6 steps without purification by column chromatography.

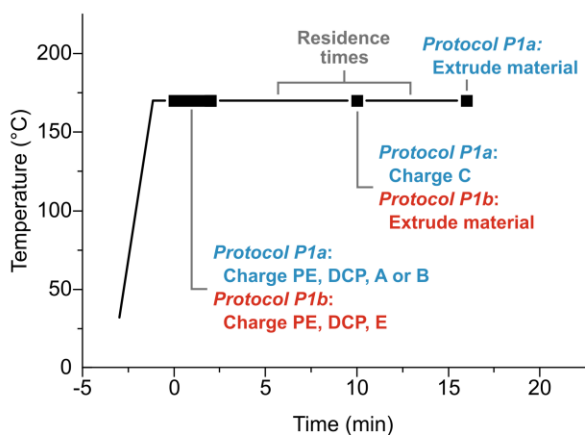
The grafting agent must also exhibit sufficient thermal stability to undergo radical-induced grafting reactions as opposed to undesired side reactions. On the basis of thermogravimetric analysis (TGA), the maleimide dioxaborolanes **A** and **B** exhibit thermal decomposition onset temperatures ( $T_{d,onset}$ ) of 227 and 238 °C, respectively (Figures S4, SI). In isothermal stability tests followed by FTIR spectroscopy (60 min at 170 °C under air or argon), pure **A** is stable under these conditions (Figures S5–S6, SI) on the basis of the constant intensity of the signal assigned to the out-of-plane C=C–H bending vibration at 830  $\text{cm}^{-1}$ . In contrast, pure **B** appears to oligomerize under argon and air; the integration of the C=O band remains essentially constant, but the intensity of the band at 830  $\text{cm}^{-1}$  decreases over time (Figures S7–S8, SI). Nevertheless, the decomposition observed for **B** does not interfere with quantitative grafting to PE under reactive extrusion conditions (vide infra). For the dimaleimide bis(dioxaborolane) **E**, a 2% mass loss is observed at a  $T_{d,onset,1}$  of 147 °C and an approximately 60% mass loss at a  $T_{d,onset,2}$  of 395 °C. Isothermal stability tests by FTIR spectroscopy as described above show that pure **E** exhibits minimal degradation under argon and air at 170 °C (Figures S9–S10, SI).

**Optimization of Reactive Grafting Protocol.** The screening of PE vitrimer synthesis was performed using the grafting agents **A+C**, **B+C**, and **E** with a targeted molar grafting density (i.e., the molar ratio of grafts to ethylene units multiplied by a factor of 1000) of 3.7, which is in line with the loadings used in previous studies on PE vitrimers.<sup>12-18,23-24</sup> The initial protocols are adapted from the one reported by our laboratory (Figure 3A).<sup>12</sup> For compositions based on

**A** and **B**, the two-step protocol **P1a** was employed in which the grafting agent and DCP (0.05 wt%) are first reacted at 170 °C with a residence time of 8 min. The crosslinker **C** is then introduced into the micro-compounder, and the material is mixed for an additional 6 min before driving it out of the mixing chamber. For compositions based on **E**, the single-step protocol **P1b** was used in which **E** and DCP (0.05 wt%) are reacted at 170 °C with a residence time of 8 min, after which the material is extruded.

The composition of all vitrimers was evaluated by FTIR spectroscopy. The complete consumption of the maleimide groups was confirmed for all materials by the complete disappearance of the out-of-plane C=C–H bending band at 830 cm<sup>-1</sup> (see Figure S11, SI, for a representative example). The molar grafting density is determined on the basis of the Beer-Lambert law (equation 1). As expected for all vitrimers, the ratio of grafts to crosslinker was found to be approximately 0.5 (equation 2). For vitrimers prepared using **A+C** and **B+C**, the quantity of the phenyl dioxaborolane units attributable to unreacted grafts and **D** that is released into the matrix is indicated by the C=C stretching bands at 1600 cm<sup>-1</sup>. The [phenyl]/[graft] ratios are calculated on the basis of equations 3 and 4.

### A. Schematic of protocols **P1a** and **P1b**



### B. Schematic of protocols **P2a**, **P2b**, and **P2c**

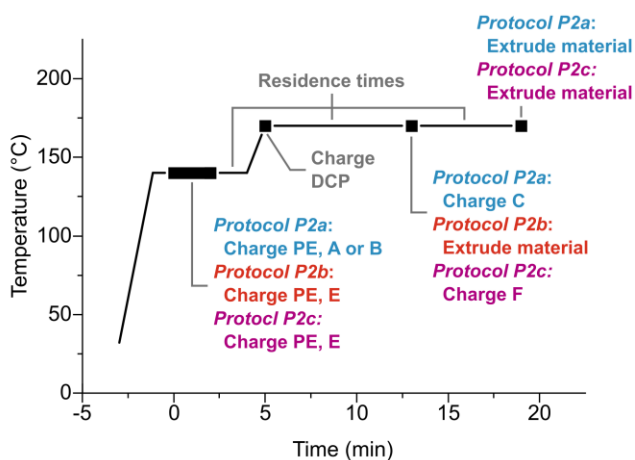


**Figure 3.** Schemes of A) protocols **P1a** and **P1b** and B) protocols **P2a**, **P2b**, and **P2c** for preparing PE vitrimers.

To quantify the fraction of grafts that are covalently attached to the polymer matrix, the materials were subjected to diolysis, which consists of de-crosslinking the vitrimers with an excess of 1,2-octanediol with respect to the number of dioxaborolane units. The composition of the de-crosslinked materials was then evaluated by FTIR spectroscopy. Successful diolysis is confirmed by the disappearance of the aromatic C=C stretching band at  $1520\text{ cm}^{-1}$  that is characteristic of the bis(dioxaborolane) crosslinker (see Figure S12, SI, for a representative example). All vitrimers prepared in this study were completely soluble in xylenes after diolysis. For clarity, the following formalism is used to name all vitrimers: those prepared from **A+C**

and **B+C** are name as  $V^x-A^yC$  and  $V^x-B^yC$ , respectively, and those prepared from **E** are named as  $V^x-E^y$ , where  $x$  is the process identification code and  $y$  is the experimentally determined molar grafting density after diolysis.

For  $V^{1a}-A^{3.6}C$  and  $V^{1a}-B^{3.4}C$  (Table 1), 5–10% of the graft content was lost after performing diolysis, indicating that a fraction of the grafting agent had undergone a side reaction and not grafted to the PE backbone. In the case of  $V^{1b}-E^{2.0}$  (Table 1), 67% of the expected quantity of **E** was detected in the as-extruded material, and only 54% of **E** was found to be grafted to the PE backbone after diolysis. Given the incompatibility of these grafting agents with the PE matrix (*vide infra*), we hypothesized that the non-quantitative grafting yield was a result of insufficient mixing with the PE matrix. Analysis of the vitrimers prepared by procedures **P1a** and **P1b** by polarized optical microscopy (POM) reveals that  $V^{1a}-B^{3.4}C$  and  $V^{1b}-E^{2.0}$  contain needle-like, phase-separated material in the vitrimer matrix (Figures S15, SI) that is not observed in the virgin PE. Although we were unable to isolate and study this additional phase, we suspect it originates from grafting agent that had undergone side reactions and not grafted onto the PE.

**Table 1.** Composition of PE vitrimers prepared by reactive extrusion.

Sample	[graft]/[ethylene] ( $\times 10^3$ ) <sup>a</sup>			Yield (%) <sup>b</sup>	[phenyl]/[graft] <sup>c</sup>	MFI (g/10 min)
	Target	As extruded	After diolysis			
V <sup>1a</sup> -A <sup>3.6</sup> C	3.7	4.1 $\pm$ 0.1	3.6 $\pm$ 0.1	96 $\pm$ 2	<0.25 <sup>d</sup>	0.05 $\pm$ 0.01 <sup>f</sup>
V <sup>1a</sup> -B <sup>3.4</sup> C	3.7	3.6 $\pm$ 0.1	3.4 $\pm$ 0.1	90 $\pm$ 1	<0.25 <sup>d</sup>	0.23 $\pm$ 0.02 <sup>f</sup>
V <sup>1b</sup> -E <sup>2.0</sup>	3.7	2.5 $\pm$ 0.1	2.0 $\pm$ 0.1	53 $\pm$ 3	n.a. <sup>e</sup>	0.23 $\pm$ 0.01 <sup>f</sup>
V <sup>2a</sup> -A <sup>3.8</sup> C	3.7	3.6 $\pm$ 0.1	3.8 $\pm$ 0.1	101 $\pm$ 1	0.28 $\pm$ 0.01	0.21 $\pm$ 0.01 <sup>g</sup>
V <sup>2a</sup> -B <sup>3.7</sup> C	3.7	3.8 $\pm$ 0.1	3.7 $\pm$ 0.1	99 $\pm$ 1	0.34 $\pm$ 0.04	1.30 $\pm$ 0.12 <sup>g</sup>
V <sup>2b</sup> -E <sup>3.8</sup>	3.7	3.7 $\pm$ 0.1	3.8 $\pm$ 0.1	101 $\pm$ 2	n.a. <sup>e</sup>	0.19 $\pm$ 0.01 <sup>f</sup> , 5.51 $\pm$ 0.17 <sup>g</sup>
V <sup>2b</sup> -E <sup>7.2</sup>	7.5	7.2 $\pm$ 0.10	7.2 $\pm$ 0.1	97 $\pm$ 1	n.a. <sup>e</sup>	0.13 $\pm$ 0.01 <sup>f</sup> , 3.37 $\pm$ 0.08 <sup>g</sup>
V <sup>2b</sup> -E <sup>10.5</sup>	11.8	11.5 $\pm$ 0.14	10.5 $\pm$ 0.1	90 $\pm$ 1	n.a. <sup>e</sup>	0.84 $\pm$ 0.04 <sup>g</sup>

<sup>a</sup>Determined by FTIR spectroscopy. <sup>b</sup>Calculated using the [graft]/[ethylene] ratios after diolysis. <sup>c</sup>Determined by FTIR spectroscopy before diolysis, where [phenyl] = [D] + [unreacted A- or B-based grafts]. <sup>d</sup>Below the level of detection. <sup>e</sup>Not applicable. <sup>f</sup>MFI determined at 190 °C with a 5.0 kg weight. <sup>g</sup>MFI determined at 190 °C with a 21.6 kg weight.

To address this issue, two new procedures, **P2a** and **P2b**, were designed to enhance the mixing of the grafting agents with the PE melt before reacting with DCP. The PE and the grafting agent are first mixed together at 140 °C, which is the lowest temperature at which this grade of PE can be mixed in the melt. After a residence time of 2 min, the temperature is increased rapidly to 170 °C, at which point the DCP is added. The remaining steps of these protocols are the same as those of **P1a** and **P1b** (Figure 3B). Gratifyingly, the use of **P2a** and **P2b** allows for the quantitative grafting for all grafting agents studied; the molar grafting density agrees with the targeted value and does not significantly decrease upon diolysis (Table 1). Of particular note is that quantitative grafting of **E** was achieved, furnishing a PE-based vitrimer in one step without any small molecule byproducts. For comparison throughout this

study, two additional vitrimers using **E** were prepared in which the target molar grafting density was increased to 7.5 and 11.8. In both cases, a grafting yield of over 90% was attained.

Interestingly, for **A+C**- and **B+C**-based vitrimers prepared by either **P1a** or **P2a**, over 65% of the expected phenyl dioxaborolane content is lost in the as-extruded vitrimer. The small molecule byproduct **D** is volatilized in the course of crosslinking, a consequence of its boiling point (235 °C at atmospheric pressure),<sup>30</sup> the high temperature of extrusion, and the presence of a nitrogen purge. This loss of **D** is implicated as an important driving force for driving the reaction between **A**- and **B**-based grafts with the crosslinker **C**.

**Viscoelastic Properties of Vitrimers.** In the absence of side reactions such as chain scission, converting a thermoplastic into a vitrimer results in an increase in viscosity. Vitrimers prepared by **P1a** and **P1b** (Table 1) exhibit MFIs that are one order of magnitude lower than that of the virgin PE (MFI = 2.49 g/10min at 190°C with 5 kg weight). Achieving higher grafting yield through the use of **P2a** and **P2b** results in a further decrease in the MFI for each respective vitrimer (Table 1). In fact, MFI measurements of **V<sup>2a</sup>-A<sup>3.8</sup>C** and **V<sup>2a</sup>-B<sup>3.7</sup>C** require a higher weight (21.6 kg instead of 5.0 kg) to conduct the MFI measurement. An intriguing observation is that **V<sup>2a</sup>-A<sup>3.8</sup>C** and **V<sup>2a</sup>-B<sup>3.7</sup>C** each exhibit a significantly lower MFI than that of **V<sup>2b</sup>-E<sup>3.8</sup>** even though they all contain the same molar grafting density. Within the series of **E**-based vitrimers, the MFI progressively decreases as the content of grafted **E** is increased (Table 1). Nevertheless, all vitrimers were driven out of the micro-compounder as smooth extrudates, and all were easily shaped by compression molding.

We probed the flow properties of PE and the vitrimers with stress relaxation experiments at 190 °C (Figure S21, SI). All materials exhibit an initial relaxation modulus of approximately 10<sup>5</sup> Pa. Unfunctionalized PE behaves like a viscoelastic liquid with a zero-shear viscosity ( $\eta_0$ ) of 3.91×10<sup>3</sup> Pa·s and a relaxation time ( $\tau$ ) of 1.35 s (equations 5 and 6). In contrast, none of the vitrimers completely relax stress, agreeing with the report of Ricarte et al.<sup>15</sup> After 3 h, **V<sup>2a</sup>-**

**A<sup>3.8</sup>C**, **V<sup>2a</sup>-B<sup>3.7</sup>C**, and **V<sup>2b</sup>-E<sup>3.8</sup>** have 4.9, 1.3, and 0.01% residual stress, respectively. In addition, the relaxation modulus does not follow a single-exponential decay for these samples, which precludes the calculation of viscosity activation energies on the basis of the Arrhenius equation.<sup>31</sup> As previously proposed,<sup>15</sup> hierarchical phase separation (vide infra) gives rise to topological constraints that prevent the system from fully relaxing stress. The formation of static crosslinks is likely not responsible for this behavior because all vitrimers are completely soluble after diolysis (vide supra).

We relied on DMA to further explore the viscoelastic properties of these materials (Figure 4). A hallmark of the transformation of a thermoplastic into a vitrimer is the presence of a rubbery plateau at temperatures above the  $T_m$  (in the case of a semi-crystalline polymer such as PE) or  $T_g$  (in the case of an amorphous polymer). In comparing vitrimers prepared by **P1a** and **P1b** (dotted lines) and **P2a** and **P2b** (solid lines), a clear increase in each respective rubbery plateau modulus is observed. This trend is consistent with an increase in the molar grafting density achieved in the optimized process for each respective vitrimer. Curiously, despite the fact that all vitrimers prepared by **P2a** and **P2b** possess the same grafting density, both **V<sup>2a</sup>-A<sup>3.8</sup>C** (solid blue line) and **V<sup>2a</sup>-B<sup>3.7</sup>C** (solid purple line) exhibit a plateau modulus of approximately 0.7 MPa (160 °C) that gradually decreases as the temperature is increased, while **V<sup>2b</sup>-E<sup>3.8</sup>** (solid red line) exhibits a plateau modulus of only 0.3 MPa (160 °C) that more sharply diminishes with increasing temperature. As the loading of **E** is increased in **V<sup>2b</sup>-E<sup>7.2</sup>** and **V<sup>2b</sup>-E<sup>10.5</sup>**, the plateau modulus reaches 0.5 and 0.9 MPa at 160 °C, respectively, although both sharply decrease with temperature. Rationalizing these distinctly different viscoelastic profiles demands a detailed description of the composition of these materials.

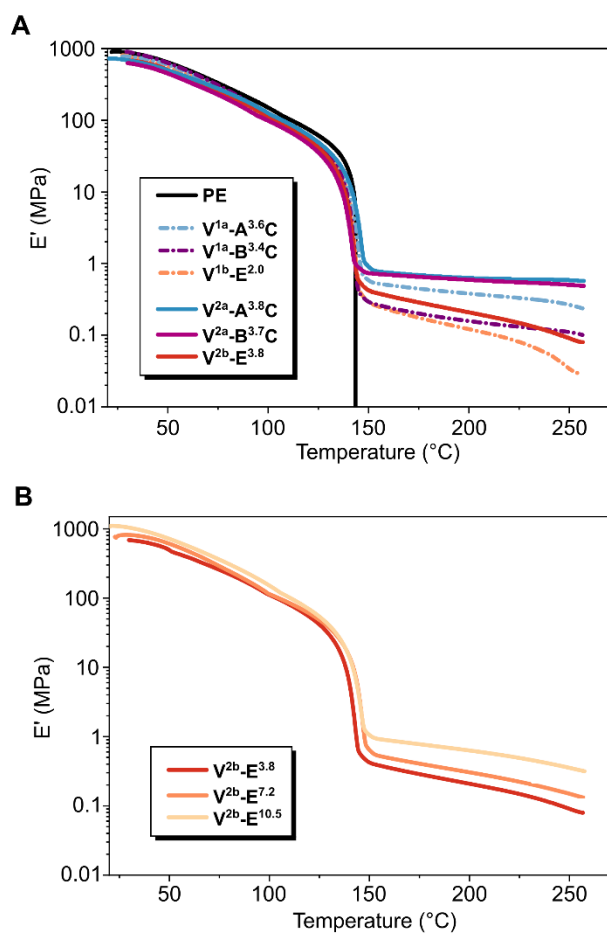


**Figure 4.** Dynamic mechanical analysis (DMA) of A) PE and vitrimers prepared from A+C, B+C, and E using either protocol P1a, P1b, P2a, or P2b. B) Vitrimers prepared with an increasing amount of E by protocol P2c.

**Composition and Viscoelastic Properties of Insoluble and Soluble Fractions.** The origin of the contrast of viscoelastic properties between A+C-, B+C-, and E-based vitrimers is illuminated by studying the composition and viscoelastic properties of the soluble and insoluble fractions. The vitrimers were boiled in xylenes overnight, and the resulting soluble and insoluble fractions were then recovered, dried, and analyzed by FTIR and DMA. The gel contents of  $V^{1a}\text{-A}^{3.6}\text{C}$ ,  $V^{1a}\text{-B}^{3.4}\text{C}$ , and  $V^{1b}\text{-E}^{2.0}$ , are found to be 35, 30, and 26% (Table 2), respectively, which is in line with previous reports from our laboratory.<sup>12-13,15</sup> By comparison, vitrimers prepared by P2a and P2b exhibit significantly higher gel contents, with increases of

at least 9% (Table 2). Vitrimers **V<sup>2b</sup>-E<sup>7.2</sup>** and **V<sup>2b</sup>-E<sup>10.5</sup>** exhibit similar gel contents of 39 and 41%, respectively.

**Table 2.** Composition of soluble and insoluble fractions and melt flow index of polyethylene vitrimers.

Sample	Gel content (%)	[graft]/[ethylene] ( $\times 10^3$ ) <sup>a</sup>		Insol./sol. ratio <sup>b</sup>
		Soluble	Insoluble	
<b>V<sup>1a</sup>-A<sup>3.6</sup>C</b>	35 ± 2	0.85 ± 0.01	8.7 ± 0.7	10
<b>V<sup>1a</sup>-B<sup>3.4</sup>C</b>	30 ± 3	0.75 ± 0.03	6.6 ± 1.8	9
<b>V<sup>1b</sup>-E<sup>2.0</sup></b>	26 ± 1	0.47 ± 0.01	8.3 ± 2.2	18
<b>V<sup>2a</sup>-A<sup>3.8</sup>C</b>	44 ± 3	1.1 ± 0.1	6.2 ± 0.2	6
<b>V<sup>2a</sup>-B<sup>3.7</sup>C</b>	47 ± 2	0.90 ± 0.03	7.2 ± 0.1	8
<b>V<sup>2b</sup>-E<sup>3.8</sup></b>	35 ± 5	0.28 ± 0.07	11 ± 1	40
<b>V<sup>2b</sup>-E<sup>7.2</sup></b>	39 ± 2	0.59 ± 0.03	20 ± 2	35
<b>V<sup>2b</sup>-E<sup>10.5</sup></b>	41 ± 1	0.26 ± 0.01	23 ± 2	90

<sup>a</sup>Determined by FTIR spectroscopy. <sup>b</sup>Ratio of [graft]/[ethylene] ratios of the insoluble and soluble fractions.

FTIR spectroscopic analyses show that the soluble fractions of all vitrimers possess a significantly reduced graft density compared to the corresponding insoluble fraction (Table 2 and Figure 5A). A striking finding is that the ratio of the grafting densities of the insoluble and soluble fractions indicates that vitrimers prepared from **E** have a more inhomogeneous composition than those prepared from **A+C** and **B+C**. For example, the vitrimers **V<sup>2a</sup>-A<sup>3.8</sup>C** and **V<sup>2a</sup>-B<sup>3.7</sup>C** exhibit an insoluble/soluble ratio of approximately 6 and 8, respectively, which are significantly lower values compared to the insoluble/soluble ratio of 40 for **V<sup>2b</sup>-E<sup>3.8</sup>**. Vitrimers with a higher content of **E** also exhibit high insoluble/soluble grafting ratios (Table 2). DMA reveals surprising consequences of the grafting inhomogeneity on the viscoelastic

properties above the  $T_m$  of the PE (Figure 5B and Figures S22, SI). The plateau moduli of the insoluble fractions of  $V^{2a}\text{-A}^{3.8}\text{C}$ ,  $V^{2a}\text{-B}^{3.7}\text{C}$ , and  $V^{2b}\text{-E}^{3.8}$  are all about 3.6 MPa at 160 °C, despite the large discrepancy between the grafting densities. In contrast, the storage moduli at 160 °C of the soluble fractions of  $V^{2a}\text{-A}^{3.8}\text{C}$  and  $V^{2a}\text{-B}^{3.7}\text{C}$  are about the same (approx. 0.3 MPa), while that of the soluble fraction of  $V^{2b}\text{-E}^{3.8}$  is significantly lower (approx. 0.1 MPa).

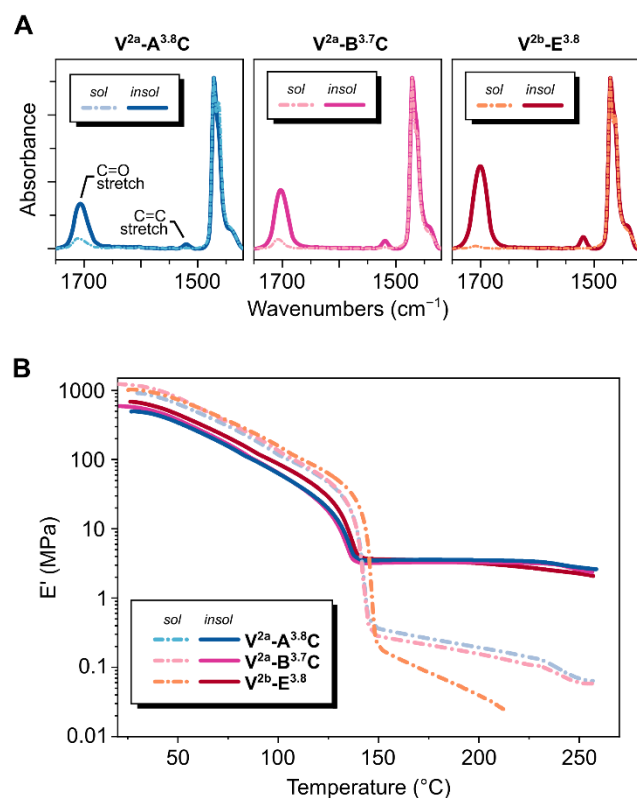


**Figure 5.** A) FTIR spectra and B) DMA of the insoluble and soluble fractions of  $V^{2a}\text{-A}^{3.8}\text{C}$ ,  $V^{2a}\text{-B}^{3.7}\text{C}$ , and  $V^{2b}\text{-E}^{3.8}$ .

The greater degree of compositional inhomogeneity of  $V\text{-E}^{3.8}$  compared to  $V^{2a}\text{-A}^{3.8}\text{C}$  and  $V^{2a}\text{-B}^{3.7}\text{C}$  is likely because **E** is less compatible with PE than **A** and **B**. This discrepancy of incompatibility is qualitatively observed in comparing the appearance of physical mixtures of molten PE with **A**, **B**, or **E** with a [maleimide]/[ethylene] ratio of 3.7 (Figure S13, SI). Like PE, mixtures with **A** and **B** are transparent at 170 °C, but the mixture with **E** is cloudy. To further test this hypothesis, we performed a model solubility test in which 10 wt% of **A**, **B**, and

**E** were each suspended in n-tetradecane and then stirred vigorously for 4 days at room temperature. Being a long linear alkane, n-tetradecane is a convenient analogue for high-density polyethylene. After the excess solids were removed using a syringe filter, the concentration of each additive was measured by FTIR spectroscopy on the basis of the intensity of the C=O stretching band at  $1710\text{ cm}^{-1}$  (Figure S14, SI). The solubilities of **A** and **B** are found to be 0.53 and 0.15 M, respectively, while the solubility of **E** is below the level of detection.

Thus, for the vitrimer compositions investigated in this study, the low solubility of **E** in PE causes a large fraction of the added **E** to graft to the molten PE at the liquid-liquid phase barrier. The improved grafting yield afforded by process **P2b** is proposed to be a consequence of forming smaller droplets of **E** in the PE melt, thereby increasing the surface area over which grafting reactions can take place. Attempts to graft more and more **E** without further changes to processing conditions, as was attempted in the synthesis of **V<sup>2b</sup>-E<sup>7.2</sup>** and **V<sup>2b</sup>-E<sup>10.5</sup>**, does not appreciably change the composition of the soluble fraction but rather augments the grafting density in the insoluble fraction.

**Thermal Stability and Crystallization Properties of Vitrimers.** The thermal stability of all materials were evaluated by thermogravimetric analysis (TGA). The unmodified PE exhibits a decomposition temperature ( $T_d$ ) of approximately  $430\text{ }^\circ\text{C}$ . Vitrimers prepared by protocol **P1a**, **V<sup>1a</sup>-A<sup>3.6</sup>C** and **V<sup>1a</sup>-B<sup>3.4</sup>C**, lose approximately 1 wt% between approximately  $150\text{ }^\circ\text{C}$  and the  $T_{d,\text{onset}}$  of PE (Figure S23, SI). This temperature range corresponds to the  $T_{d,\text{onset}}$  values observed for **A** and **B**, respectively (Figure S4A,B, SI). In contrast, **V<sup>1b</sup>-E<sup>2.0</sup>** does not exhibit any mass loss below  $430\text{ }^\circ\text{C}$  despite it containing a significant fraction of ungrafted material, but this behavior is likely because **E** has a  $T_d$  that is similar to that of PE (Figure S4C, SI). All vitrimers prepared by protocols **P2a** and **P2b** show no sign of premature degradation (Figure S24, SI), representing another benefit of achieving quantitative grafting using the

optimized protocols. These results also highlight the improved stability of the maleimide-derived grafts compared to the nitroxide-based grafts that have been previously reported.<sup>14</sup>

Compared to PE, all vitrimers exhibit a similar melting transition temperature (Figure S25, SI) but a lower degree of crystallinity on the basis of DSC (Table 3). The percent crystallinity values measured by DSC agree with those measured by powder X-ray diffraction (XRD, Table S4, SI). In general, increasing the grafting density results in a decrease in percent crystallinity; however, the graft density of the soluble and insoluble fractions must be considered in this analysis (Table S2, SI). The vitrimer **V<sup>2b</sup>-E<sup>3.8</sup>** exhibits a higher degree of crystallinity than **V<sup>2a</sup>-A<sup>3.8</sup>C** and **V<sup>2a</sup>-B<sup>3.7</sup>C** despite having a similar grafting density. This characteristic is likely a result of **V<sup>2b</sup>-E<sup>3.8</sup>** containing a larger proportion of highly crystalline graft-poor material compared to **V<sup>2a</sup>-A<sup>3.8</sup>C** and **V<sup>2a</sup>-B<sup>3.7</sup>C**.

**Table 3.** Thermal properties PE vitrimers measured by DSC.

Sample	$\chi_c$ (%)	$T_m$ (°C)	$T_c$ (°C)
PE	60.1 ± 0.7	127.5 ± 0.2	113.2 ± 0.2
<b>V<sup>2a</sup>-A<sup>3.8</sup>C</b>	53.4 ± 0.1	126.8 ± 0.1	114.3 ± 0.1
<b>V<sup>2a</sup>-B<sup>3.7</sup>C</b>	53.6 ± 0.7	127.0 ± 0.1	114.4 ± 0.3
<b>V<sup>2b</sup>-E<sup>3.8</sup></b>	56.0 ± 0.1	128.4 ± 0.1	115.7 ± 0.1
<b>V<sup>2b</sup>-E<sup>7.2</sup></b>	56.7 ± 0.2	128.5 ± 0.1	114.7 ± 0.2
<b>V<sup>2b</sup>-E<sup>10.5</sup></b>	53.8 ± 0.6	128.0 ± 0.1	114.6 ± 0.2

A peculiar feature of these vitrimers is that they all exhibit higher  $T_c$  values compared to PE (Figure S26, SI). The observed increase in  $T_c$  (e.g., 2.5 °C in the case of **V<sup>2b</sup>-E<sup>3.8</sup>**) is corroborated by comparable increases to  $T_c$  values for similar PE-based vitrimers reported by Ricarte et al.<sup>13</sup> Augmentation of the  $T_c$  of this magnitude is significant, as it is in line with

increases realized when using nucleating agents in PE.<sup>32</sup> This finding is unexpected not only because the crystallization temperature of PE is suppressed when non-dynamically crosslinked by DCP,<sup>33</sup> but also because the soluble and insoluble fractions exhibit lower  $T_c$  values compared to that of each respective vitrimer (Table S2, SI). For example, the  $T_c$  values of the soluble and insoluble fractions of **V<sup>2b</sup>-E<sup>3.8</sup>** are  $115.0 \pm 0.1$  and  $113.3 \pm 0.1$  °C (Table S2, SI), respectively, which are both less than the  $T_c$  of  $115.7 \pm 0.1$  °C for **V<sup>2b</sup>-E<sup>3.8</sup>** (Table 3). These results imply that the dioxaborolane-rich regions act as a nucleating agent for the PE, although this effect appears to be tied to the hierarchical features introduced by the vitrimers.

**Hierarchical Structure of Vitrimers.** The macroscopic morphology of the virgin PE and the vitrimers were investigated by polarized optical microscopy (POM). Melting and crystallization transition temperatures observed by POM (Table S1, SI) are systematically higher than those recorded by DSC, likely a result of the slower heating and cooling rates used for these experiments ( $5$  °C·min<sup>-1</sup> for POM vs.  $10$  °C·min<sup>-1</sup> for DSC). After cooling from the melt, unmodified PE forms large spherulites of approximately  $25$   $\mu\text{m}$  in diameter with polygonal shapes as a result of impingement (Figure 6A and Figure S16–S17, SI). The spherulites are readily identified by the Maltese cross and optical banding patterns. Vitrimers produced by protocol **P2a** and **P2b** form spherulites that are smaller than  $5$   $\mu\text{m}$  upon cooling from the melt, appearing as a halo of birefringence across each sample (Figures S17–S20, SI). At higher magnification, as in the micrographs presented in Figure 6B,C, the vitrimers adopt a fine speckled texture with crossed polarizers, which we attribute to the Maltese cross pattern of the numerous small spherulites. Interestingly, we observe two distinct regions in all vitrimer samples—one region features the finely speckled birefringent texture described above, and the other region exhibits a smooth, featureless texture. Qualitatively, these two regions are more coarsely intermixed in **V<sup>2a</sup>-A<sup>3.8</sup>C** and **V<sup>2a</sup>-B<sup>3.7</sup>C** compared to **V<sup>2b</sup>-E<sup>3.8</sup>**.

Nanoscale features were probed by small-angle X-ray diffraction experiments (SAXS) and XRD. All measurements were conducted at ambient temperature, and thus all samples were in the semi-crystalline state. The SAXS patterns of the virgin PE and the vitrimers essentially overlap at high  $q$ , as they all exhibit the crystal lamellae structure factor of PE (Figure 7A). Any nanoscale features unique to the vitrimers in this size regime are thus obscured. Although no peaks are observed at low  $q$ , an increase in the scaling factor [i.e., the slope of  $I(q)$  versus the wavevector  $q$  in a log-log plot] is observed going from PE to  $V^{2a}\text{-A}^{3.8}\text{C}$  to  $V^{2a}\text{-B}^{3.7}\text{C}$  and finally to  $V^{2b}\text{-E}^{3.8}$ . Samples of  $V^{2b}\text{-E}^{7.2}$  and  $V^{2b}\text{-E}^{10.5}$  have scattering patterns that closely match that of  $V^{2b}\text{-E}^{3.8}$  but with higher intensity scattering at low  $q$  (Figure 7B).

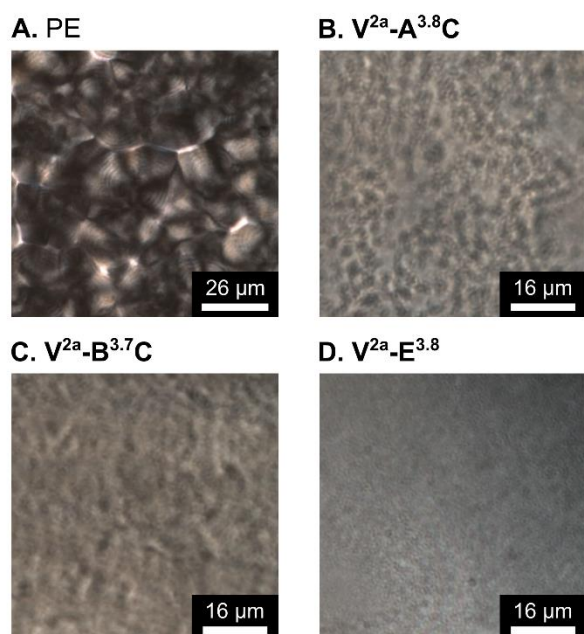


**Figure 6.** Polarized optical microscopy images (crossed polarizers) of A) PE, B)  $V^{2a}\text{-A}^{3.8}\text{C}$ , C)  $V^{2a}\text{-B}^{3.7}\text{C}$ , and D)  $V^{2a}\text{-E}^{3.8}$  at room temperature after cooling from the melt (full images are presented in Figures S18–S20, SI).

As previously reported,<sup>13</sup> scattering at low  $q$  for PE vitrimers can be attributed to fractal assemblies of aggregates of the grafted dioxaborolane units, which are described by both a fractal length scale ( $\zeta$ ) and a fractal dimension ( $D$ ). The increase in scattering intensity at low

$q$  but the absence of a peak suggests that fractal objects are also formed in  $V^{2a}\text{-A}^{3.8}\text{C}$ ,  $V^{2a}\text{-B}^{3.7}\text{C}$ , and  $V^{2b}\text{-E}^{3.8}$ , but that  $\zeta$  for these samples falls outside the range measurable by SAXS (i.e., greater than 200 nm). However,  $D$  can be estimated by the slope of the linear region (in a log-log plot) observed over approximately a decade at low  $q$ .<sup>34</sup> Thus,  $D$  for  $V^{2a}\text{-A}^{3.8}\text{C}$ ,  $V^{2a}\text{-B}^{3.7}\text{C}$ , and  $V^{2b}\text{-E}^{3.8}$  increases from approximately 2.2 to 2.3 to 2.6, respectively. Both  $V^{2b}\text{-E}^{7.2}$  and  $V^{2b}\text{-E}^{10.5}$  exhibit a  $D$  of approximately 2.6, matching that of  $V^{2b}\text{-E}^{3.8}$ . The trend of increasing fractal dimension going from **A**- to **B**- to **E**-based vitrimers is inversely correlated to the miscibility of the corresponding grafting agent in PE (vide supra). This relationship suggests that decreasing miscibility of the grafting agent results in more compact clusters of grafts in the matrix. It must be noted that  $V^{2a}\text{-A}^{3.8}\text{C}$  and  $V^{2a}\text{-B}^{3.7}\text{C}$  both contain some small molecule byproduct **D**, which may be expected to affect  $D$ . We probed this question in further SAXS experiments with **E**-based vitrimers that are loaded with varying amounts of a reactive processing aid that has a structure similar to that of **D** (vide infra). As can be seen in Figure S28 (SI),  $D$  is not strongly influenced by increasing the loading of **F**.

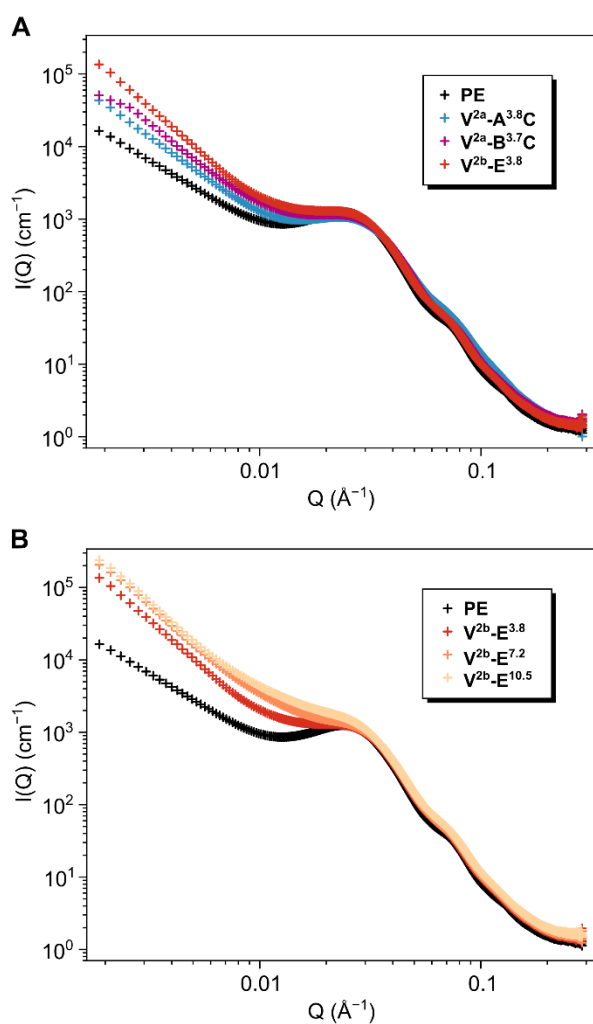


**Figure 7.** Small-angle X-ray scattering patterns for A) PE,  $V^{2a}\text{-A}^{3.8}\text{C}$ ,  $V^{2a}\text{-B}^{3.7}\text{C}$ , and  $V^{2b}\text{-E}^{3.8}$ , and B) PE,  $V^{2b}\text{-E}^{3.8}$ ,  $V^{2b}\text{-E}^{7.2}$ , and  $V^{2b}\text{-E}^{10.5}$ .

The unit cell parameters of vitrimers prepared using **A**, **B**, and **E** are nearly identical to those of virgin PE on the basis of XRD (Figure S27 and Table S4, SI). Moreover, application of the Scherrer equation (equation 9) to the peak widths of the reflections corresponding to the (110) and (200) planes of the PE crystal unit cell reveals that the crystallite size is approximately the same for the vitrimers and virgin PE (Table S4, SI). The lamellar dimensions were also calculated by converting the SAXS patterns into electron density correlation functions (Table S5, SI). These measurements further indicate that the crystal structure of PE is not strongly perturbed by any of the dioxaborolane grafting units considered in this study.

**Mechanical Properties.** The mechanical properties of virgin PE and vitrimers prepared by **P2a** and **P2b** were evaluated by performing tensile tests at room temperature. The stress-strain curves are presented Figure 8A, and the corresponding mechanical properties are presented in Figure 8B (see Table S6, SI, for tabulated values). The grade of PE used in this study exhibits typical ductile behavior, featuring a well-defined yield point, a stable drawing zone, and a final strain-hardening region before rupture. The vitrimers display similar ductile behavior and largely perform as expected for lightly crosslinked PE. Given that these tests were performed at room temperature, metathesis between the dioxaborolane crosslinking units is slow, and thus these linkages behave like non-dynamic crosslinks. The vitrimers all exhibit a smaller drawing zone, resulting in an overall reduction to the percent elongation at break (792% for PE compared to 600–661% for the vitrimers). The vitrimers have a similarly sized strain hardening region but with a larger slope before rupture compared to PE. The stress at break of PE ( $27 \pm 2$  MPa) and the vitrimers are all similar in value, with only **V<sup>2b</sup>-E<sup>10.5</sup>** exhibiting a stress at break ( $32.5 \pm 0.8$ ) that is significantly higher than that of PE.

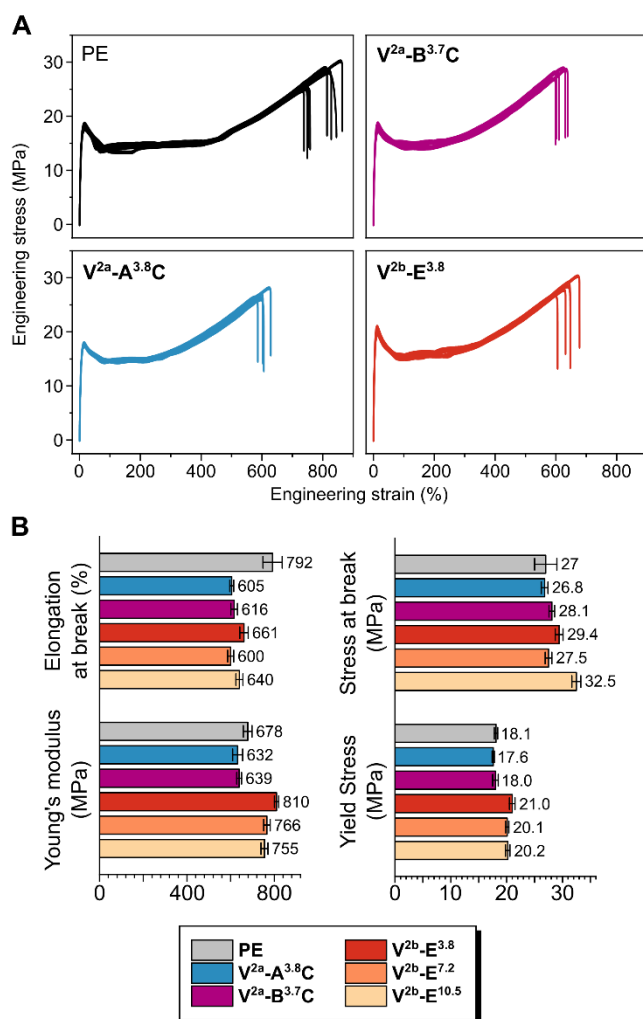


**Figure 8.** A) Stress-strain curves of virgin PE and vitrimers acquired at room temperature and B) calculated mechanical properties.

A notable peculiarity lies in the elastic response of the **E**-based vitrimers. The Young's moduli and the yield stress values of V<sup>2b</sup>-E<sup>3.8</sup>, V<sup>2b</sup>-E<sup>7.2</sup>, and V<sup>2b</sup>-E<sup>10.5</sup> are all significantly higher compared to that of PE, in contrast to the inferior elastic response observed for V<sup>2a</sup>-A<sup>3.8</sup>C and V<sup>2a</sup>-B<sup>3.7</sup>C. As a comparison, both the Young's modulus and the yield stress have been found to increase monotonically with the percent crystallinity of PE that is lightly crosslinked with organic peroxides.<sup>35</sup> At low stress, the crosslinking density of these peroxide-crosslinked PE samples do not clearly correlate with the elastic properties. In the present case, it is surprising that the **E**-based vitrimers exhibit enhanced elastic properties despite having a lower percent

crystallinity compared to unmodified PE (e.g., 60% crystallinity for PE and 56% crystallinity for  $V^{2b}$ -E<sup>3.8</sup>, Table 3). We suspect that the presence of the small molecule **D** in  $V^{2a}$ -A<sup>3.8</sup>C and  $V^{2a}$ -B<sup>3.7</sup>C could be an important contributor to their inferior elastic properties compared to those of  $V^{2b}$ -E<sup>3.8</sup> (vide infra).

**Modulating Mechanical Properties with a Reactive Processing Aid.** Processing aids are commonly employed in polyolefin resins to lower the melt viscosity, which decreases the time and energy needed for processing (e.g., filling a mold).<sup>36</sup> They are typically small molecules that are at least partially miscible with the polymer melt, and they essentially lubricate polymer chains sliding past one another. We envision that reactive processing aids for polyolefin vitrimers would be particularly effective if they contain a functional group that can interact with the dynamic covalent linkages. For example, introducing a mono-functional compound to an E-based vitrimer is expected to compete with the formation of crosslinks as schematically depicted in Figure 9.<sup>37</sup> It is anticipated to reduce the crosslinking density as well as facilitate exchange reactions due to the higher rate of diffusion of the processing aids compared to the polymer chains. Both phenomena will increase the ability of the vitrimer to flow.

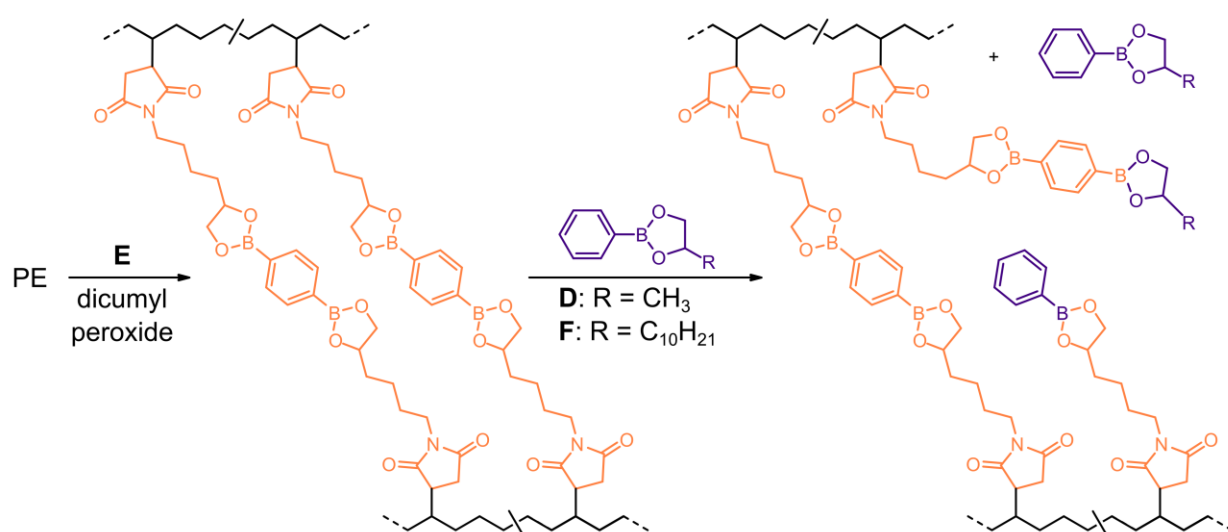


**Figure 9.** Synthesis of E-based PE vitrimers that contain **F** as a reactive processing aid.

The small molecule byproduct **D** described above in principle acts in this way (Figure 9, R = CH<sub>3</sub>), but it is not practically useful as a reactive processing aid because the free molecule evaporates from the melt during reactive grafting (*vide supra*). We instead employed compound **F** (Figure 9, R = C<sub>10</sub>H<sub>21</sub>) to exemplify a reactive processing aid in a vitrimer because of its lower volatility. A series of **E**-based vitrimers were thus prepared using protocol **P2c**, which is essentially **P2b** with an additional step before extrusion in which **F** is introduced and mixed in the melt (Figure 3B). Four vitrimers were prepared with approximately 11 grafts per 10<sup>3</sup> ethylene units, and they were loaded with varying amounts of **F** (Table 4). Two samples of unmodified PE were also loaded with **F** for comparison. Quantification of **F** was experimentally determined by FTIR spectroscopy of the extruded vitrimer on the basis of the C=C stretching band of the phenyl dioxaborolane units at 1600 cm<sup>-1</sup> (equations 3 and 4). The vitrimers are identified as **V<sup>2c</sup>-E<sup>x</sup>-F<sup>y</sup>** and the PE samples are named as **PE-F<sup>y</sup>**, where *x* is the experimental graft density of the as-extruded material and *y* is the experimentally-determined ratio of **F** per 10<sup>3</sup> ethylene units. It is important to note that unreacted and reacted **F** cannot be distinguished on the basis of FTIR spectroscopy, and thus *y* is defined as the sum of these species.

**Table 4.** Composition and MFI of **E**-based vitrimers loaded with varying amounts of **F**.

Sample	[F]/[graft] <sup>a</sup>	Average crosslink density <sup>b</sup>	Average number of crosslinks per chain <sup>c</sup>	Gel content (%)	Insol./sol. ratio <sup>d</sup>	MFI (g/10min) <sup>e</sup>
PE	n.a. <sup>f</sup>	n.a. <sup>f</sup>	n.a. <sup>f</sup>	n.a. <sup>f</sup>	0	2.49 ± 0.01
PE-F <sup>3.9</sup>	n.a. <sup>f</sup>	n.a. <sup>f</sup>	n.a. <sup>f</sup>	n.a. <sup>f</sup>	n.a. <sup>f</sup>	3.18 ± 0.08
PE-F <sup>12.8</sup>	n.a. <sup>f</sup>	n.a. <sup>f</sup>	n.a. <sup>f</sup>	n.a. <sup>f</sup>	n.a. <sup>f</sup>	3.78 ± 0.09
V <sup>2b</sup> -E <sup>10.5</sup>	n.a. <sup>f</sup>	5.25	6.63	41 ± 1	90	0.84 ± 0.04 <sup>g</sup>
V <sup>2c</sup> -E <sup>11.4</sup> -F <sup>1.7</sup>	0.15 ± 0.02	4.2	5.45	42 ± 3	67	0.09 ± 0.01
V <sup>2c</sup> -E <sup>11.1</sup> -F <sup>2.9</sup>	0.26 ± 0.06	3.49	4.40	41 ± 3	49	0.17 ± 0.01
V <sup>2c</sup> -E <sup>11.2</sup> -F <sup>7.2</sup>	0.65 ± 0.20	2.07	2.62	37 ± 4	15	0.37 ± 0.02
V <sup>2c</sup> -E <sup>10.7</sup> -F <sup>16.7</sup>	1.6 ± 0.1	0.89	1.03	29 ± 1	14	1.05 ± 0.03

<sup>a</sup>Determined by FTIR spectroscopy. <sup>b</sup>Calculated per 10<sup>3</sup> ethylene units according to equation 13. <sup>c</sup>Calculated based on the degree of polymerization (DP<sub>n</sub> = 1260) of the PE used in this study. <sup>d</sup>Ratio of [graft]/[ethylene] ratios of the insoluble and soluble fractions (see Table S7, SI). <sup>e</sup>MFI determined at 190°C with 5 kg weight unless noted otherwise. <sup>f</sup>Not applicable. <sup>g</sup>MFI determined at 190 °C with a 21.6 kg weight.

The concentration of **F** modulates the average connectivity of the vitrimers. As the content of **F** is increased, the average crosslinking density for a given grafting of **E** is decreased (Table 4 and equations 10–12). As a consequence, the functionality of the polymer chains found in the soluble fraction increases with **F** content, and the disparity in the graft density between the soluble and insoluble phases decreases (Table 4). We also attribute these observed shifts in composition to **F** acting as a reactive compatibilizer between the graft rich and graft poor domains. It must be emphasized that the addition of **F** does not influence the homogeneity of grafting along the polymer chain because **F** is added only after the radical-initiated reaction of **E** with the PE.

Remarkably, the gel content is essentially the same (approximately 40%) for the vitrimers V<sup>2c</sup>-E<sup>10.5</sup>, V<sup>2c</sup>-E<sup>11.4</sup>-F<sup>1.7</sup>, V<sup>2c</sup>-E<sup>11.1</sup>-F<sup>2.9</sup> and V<sup>2c</sup>-E<sup>11.2</sup>-F<sup>7.2</sup>, while the crosslinking density is

decreased by a factor of ca. 2.5 when going from  $V^{2c}\text{-E}^{10.5}$  to  $V^{2c}\text{-E}^{11.2}\text{-F}^{7.2}$ , a consequence of the addition of an increasing amount of **F**. The fact that the gel content does not appreciably change across these samples is consistent with heterogeneous distribution of **E**-based crosslinks in the PE matrix. This is further confirmed by the high gel content of vitrimer  $V^{2c}\text{-E}^{10.7}\text{-F}^{16.7}$  (29%) given that this sample only contains approximately one crosslink per chain on average (Table 4).

The changes in composition induced by **F** give rise to important changes to the thermomechanical properties of the vitrimers. The control experiments suggest that **F** also behaves like a processing aid in unfunctionalized PE. For both the vitrimers and unfunctionalized PE, increasing the loading of **F** causes the melt flow index to increase (Table 4). Increasing the loading of **F** in vitrimers also results in an increased rate of stress relaxation (Figure S21B). By DMA, the vitrimers exhibit a storage modulus above the  $T_m$  of the PE matrix that decreases as the concentration of **F** increases, ranging from 0.6 MPa for  $V^{2c}\text{-E}^{11.4}\text{-F}^{1.7}$  to 0.2 MPa for  $V^{2c}\text{-E}^{10.7}\text{-F}^{16.7}$  at 160 °C (Figure 10A). We would like to highlight that despite  $V^{2c}\text{-E}^{10.7}\text{-F}^{16.7}$  having such a high loading of **F** (1.6 equivalents of **F** per graft) and thus a low average graft density (1.03 grafts per chain, Table 4), it still exhibits a storage modulus above the  $T_m$ . The tensile properties of the **E**-based vitrimers and unfunctionalized PE are also strongly influenced by the presence of **F** (Figure 10B and Table S6, SI). As the content of **F** is increased, both series of materials become less stiff, and the elongation at break is significantly increased. These results suggest that the flow and mechanical properties of a given vitrimer composition can be effectively tuned using a reactive processing aid.

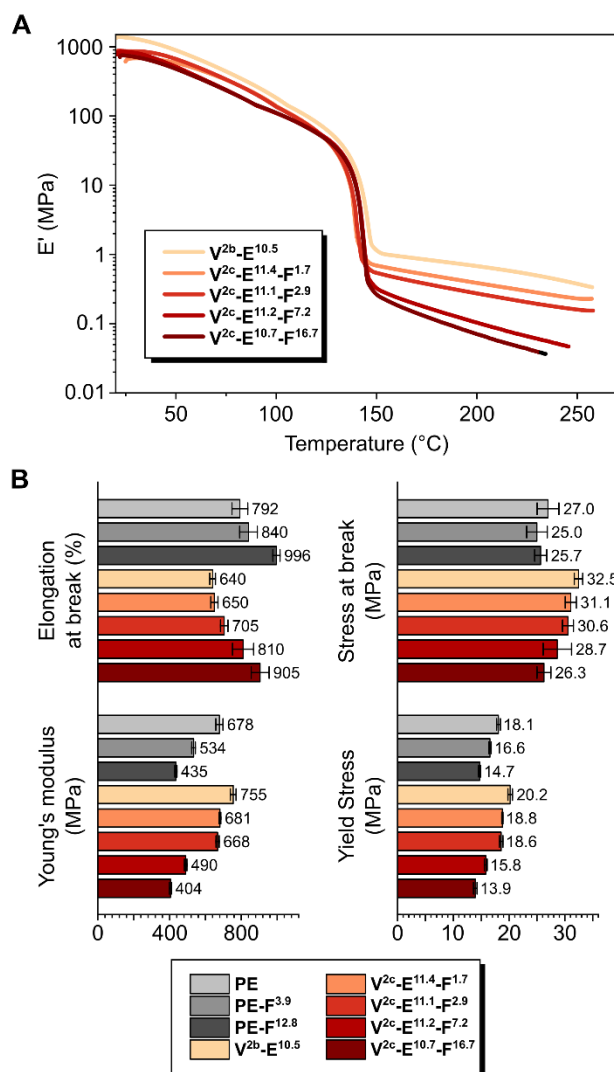


**Figure 10.** DMA of PE and **E**-based vitrimers loaded with varying amounts of **F**.

## Conclusion

The design of the dimaleimide bis(dioxaborolane) **E** permits access to PE vitrimers in one step via reactive extrusion without the release of a small molecule byproduct. The resulting **E**-based vitrimers exhibit thermal stability that is comparable to that of virgin PE, allowing it to be easily (re)processed by extrusion or compression molding. Moreover, the **E**-based vitrimers feature superior tensile properties compared to comparable PE vitrimers prepared using either **A+C** or **B+C**. To achieve this level of performance, it is necessary to quantitatively graft the

additives to the PE backbone, which requires that the grafting agents be efficiently mixed in the molten PE before initiating the grafting reaction with an organic peroxide.

Small changes to the structure of the grafting agent have important consequences on the composition and flow properties of the resulting vitrimers. For instance, despite similar overall grafting densities, **E**-based vitrimers exhibit a significantly larger ability to flow in the melt compared to those derived from **A** and **B**. This peculiar feature is traced to the lower gel content and the lower degree of grafting density in the soluble phase of the **E**-based vitrimers. The soluble phase essentially acts as a lubricant for the insoluble phase, and its comparatively lower grafting density enhances the ability of **E**-based vitrimers to flow. The compositional discrepancy between **A+C**-, **B+C**-, and **E**-based vitrimers are ultimately due to differences in the compatibility of the different grafting agents in the PE melt. Since **E** is less compatible than **A** and **B**, it results in vitrimers that exhibit a greater degree of compositional inhomogeneity.

The discrepancies in the insoluble/soluble grafting density ratios impact the structural and morphological features of the resulting vitrimers ranging from the nano- to the macroscale. Although neither the crystal structure nor the crystallite size of PE are significantly perturbed by the presence of the dynamic crosslinks, the compactness of the nanoscale clusters of the grafted units depends on the miscibility of the grafting agent with PE on the basis of SAXS. On the macroscale, it is clear that **E**-based vitrimers present a more homogeneous mixing of the spherulite-poor and spherulite-rich macrophases than in **A+C** and **B+C**-based vitrimers, which is likely a consequence of the larger fraction of soluble material in the **E**-based vitrimers.

In addressing the challenge of synthesizing vitrimers that are easily processable,<sup>6,38-41</sup> the present work highlights how incompatibility effects can be harnessed to make heterogeneous materials that have a high gel content but can still readily flow. The modulation of the compatibility of the grafting agent in the polymer matrix during reactive processing represents a powerful tool for controlling the degree of heterogeneity of the resulting polymer network.

We hope that this work will serve not only as a basis for future research on PE vitrimers but also as an inspiration for the design of grafting agents that provide direct access to easily-processable vitrimers.

## ASSOCIATED CONTENT

Additional experiments and raw data are provided in the Supporting Information. This material is available free of charge via the Internet at <http://pubs.acs.org>.

## AUTHOR INFORMATION

### **Corresponding Author**

\* E-mail: [nathan.van-zee@espci.psl.eu](mailto:nathan.van-zee@espci.psl.eu) and [renaud.nicolay@espci.psl.eu](mailto:renaud.nicolay@espci.psl.eu)

### **Author Contributions**

The manuscript was written through contributions of all authors. All authors have given approval to the final version of the manuscript.

## ACKNOWLEDGMENT

M. M. acknowledges Thomas Vialon for his assistance in performing GC-MS analyses. The authors acknowledge the City of Paris for funding through the Paris Emergence program and Aliaxis R&D for financial support. The authors acknowledge SOLEIL for the provision of synchrotron radiation facilities on the beamline SWING. This work benefited from the use of the SasView application, originally developed under NSF award DMR-0520547. SasView

contains code developed with funding from the European Union's Horizon 2020 research and innovation program under the SINE2020 project, grant agreement No 654000.

## REFERENCES

1. Denissen, W.; Winne, J. M.; Du Prez, F. E., Vitrimers: permanent organic networks with glass-like fluidity. *Chem. Sci.* **2016**, *7*, 30-38.
2. Fortman, D. J.; Brutman, J. P.; De Hoe, G. X.; Snyder, R. L.; Dichtel, W. R.; Hillmyer, M. A., Approaches to Sustainable and Continually Recyclable Cross-Linked Polymers. *ACS Sust. Chem. Eng.* **2018**, *6*, 11145-11159.
3. Zhang, Z. P.; Rong, M. Z.; Zhang, M. Q., Polymer engineering based on reversible covalent chemistry: A promising innovative pathway towards new materials and new functionalities. *Prog. Polym. Sci.* **2018**, *80*, 39-93.
4. Chakma, P.; Konkolewicz, D., Dynamic Covalent Bonds in Polymeric Materials. *Angew. Chem., Int. Ed.* **2019**, *58*, 9682-9695.
5. Scheutz, G. M.; Lessard, J. J.; Sims, M. B.; Sumerlin, B. S., Adaptable Crosslinks in Polymeric Materials: Resolving the Intersection of Thermoplastics and Thermosets. *J. Am. Chem. Soc.* **2019**, *141*, 16181-16196.
6. Van Zee, N. J.; Nicolay, R., Vitrimers: Permanently crosslinked polymers with dynamic network topology. *Prog. Polym. Sci.* **2020**, *104*, 101233.
7. Guerre, M.; Taplan, C.; Winne, J. M.; Du Prez, F. E., Vitrimers: directing chemical reactivity to control material properties. *Chem. Sci.* **2020**, *11*, 4855-4870.
8. Montarnal, D.; Capelot, M.; Tournilhac, F.; Leibler, L., Silica-Like Malleable Materials from Permanent Organic Networks. *Science* **2011**, *334*, 965-968.
9. Capelot, M.; Montarnal, D.; Tournilhac, F.; Leibler, L., Metal-Catalyzed Transesterification for Healing and Assembling of Thermosets. *J. Am. Chem. Soc.* **2012**, *134*, 7664-7667.

10. Capelot, M.; Unterlass, M. M.; Tournilhac, F.; Leibler, L., Catalytic Control of the Vitrimer Glass Transition. *ACS Macro Lett.* **2012**, *1*, 789-792.
11. Lamm, M. E.; Wang, Z.; Zhou, J.; Yuan, L.; Zhang, X.; Tang, C., Sustainable epoxy resins derived from plant oils with thermo- and chemo-responsive shape memory behavior. *Polymer* **2018**, *144*, 121-127.
12. Röttger, M.; Domenech, T.; van der Weegen, R.; Breuillac, A.; Nicolaÿ, R.; Leibler, L., High-performance vitrimers from commodity thermoplastics through dioxaborolane metathesis. *Science* **2017**, *356*, 62-65.
13. Ricarte, R. G.; Tournilhac, F.; Leibler, L., Phase Separation and Self-Assembly in Vitrimers: Hierarchical Morphology of Molten and Semicrystalline Polyethylene/Dioxaborolane Maleimide Systems. *Macromolecules* **2019**, *52*, 432-443.
14. Caffy, F.; Nicolay, R., Transformation of polyethylene into a vitrimer by nitroxide radical coupling of a bis-dioxaborolane. *Polym. Chem.* **2019**, *10*, 3107-3115.
15. Ricarte, R. G.; Tournilhac, F.; Cloitre, M.; Leibler, L., Linear Viscoelasticity and Flow of Self-Assembled Vitrimers: The Case of a Polyethylene/Dioxaborolane System. *Macromolecules* **2020**, *53*, 1852-1866.
16. Ji, F.; Liu, X.; Lin, C.; Zhou, Y.; Dong, L.; Xu, S.; Sheng, D.; Yang, Y., Reprocessable and Recyclable Crosslinked Polyethylene with Triple Shape Memory Effect. *Macromol. Mater. Eng.* **2019**, *304*, 1800528.
17. Zych, A.; Pinalli, R.; Soliman, M.; Vachon, J.; Dalcanale, E., Polyethylene vitrimers via silyl ether exchange reaction. *Polymer* **2020**, *199*, 122567.
18. Tellers, J.; Pinalli, R.; Soliman, M.; Vachon, J.; Dalcanale, E., Reprocessable vinylogous urethane cross-linked polyethylene via reactive extrusion. *Polym. Chem.* **2019**, *10*, 5534-5542.

19. Beyer, G.; Hopmann, C., *Reactive Extrusion: Principles and Applications*. Wiley-VCH: Weinheim, Germany, 2018.
20. Moad, G., The synthesis of polyolefin graft copolymers by reactive extrusion. *Prog. Polym. Sci.* **1999**, *24*, 81-142.
21. Hall, D. G., *Boronic Acids: Preparation, Applications in Organic Synthesis and Medicine*. Wiley-VCH: Weinheim, 2005; p 545.
22. Martin, R.; Buchwald, S. L., Palladium-Catalyzed Suzuki-Miyaura Cross-Coupling Reactions Employing Dialkylbiaryl Phosphine Ligands. *Acc. Chem. Res.* **2008**, *41*, 1461-1473.
23. Tanaka, R.; Tonoko, N.; Kihara, S.-i.; Nakayama, Y.; Shiono, T., Reversible star assembly of polyolefins using interconversion between boroxine and boronic acid. *Polym. Chem.* **2018**, *9*, 3774-3779.
24. Yang, F.; Pan, L.; Ma, Z.; Lou, Y.; Li, Y.; Li, Y., Highly elastic, strong, and reprocessable cross-linked polyolefin elastomers enabled by boronic ester bonds. *Polym. Chem.* **2020**, *11*, 3285-3295.
25. Wunderlich, B., *Macromolecular Physics, Vol. 2*. Academic Press: New York, 1973.
26. Murthy, N. S., X-Ray Diffraction from Polymers. In *Polymer Morphology*, Guo, Q., Ed. John Wiley & Sons, Inc: Hoboken, NJ, USA, 2016; pp 14–36.
27. Klug, H. P.; Alexander, L. E., *X-Ray Diffraction Procedures: For Polycrystalline and Amorphous Materials*. 2nd ed.; Wiley: New York, 1974.
28. German, I.; D'Agosto, F.; Boisson, C.; Tencé-Girault, S.; Soulié-Ziakovic, C., Microphase Separation and Crystallization in H-Bonding End-Functionalized Polyethylenes. *Macromolecules* **2015**, *48*, 3257-3268.

29. Yan, P.; Zhao, W.; Fu, X.; Liu, Z.; Kong, W.; Zhou, C.; Lei, J., Multifunctional polyurethane-vitrimers completely based on transcarbamoylation of carbamates: thermally-induced dual-shape memory effect and self-welding. *RSC Adv.* **2017**, *7*, 26858-26866.
30. Finch, A.; Lockhart, J. C., 721. Cyclic boronates and their amine complexes. *J. Chem. Soc.* **1962**, 3723-3726
31. Scheutz, G. M.; Lessard, J. J.; Sims, M. B.; Sumerlin, B. S., Adaptable Crosslinks in Polymeric Materials: Resolving the Intersection of Thermoplastics and Thermosets. *J. Am. Chem. Soc.* **2019**, *141*, 16181-16196.
32. Seven, K. M.; Cogen, J. M.; Gilchrist, J. F., Nucleating agents for high-density polyethylene-A review. *Polymer Engineering and Science* **2016**, *56*, 541-554.
33. Kao, Y. H.; Phillips, P. J., Crystallinity in chemically crosslinked low density polyethylenes: 1. Structural and fusion studies. *Polymer* **1986**, *27*, 1669-1678.
34. Lazzari, S.; Nicoud, L.; Jaquet, B.; Lattuada, M.; Morbidelli, M., Fractal-like structures in colloid science. *Adv. Colloid. Interface Sci.* **2016**, *235*, 1-13.
35. Pérez, C. J.; Cassano, G. A.; Vallés, E. M.; Quinzani, L. M.; Failla, M. D., Tensile mechanical behavior of linear high-density polyethylenes modified with organic peroxide. *Polym. Eng. Sci.* **2003**, *43*, 1624-1633.
36. Tolinski, M., *Additives for Polyolefins: Getting the most out of Polypropylene, Polyethylene, and TPO*. Elsevier: Burlington, MA, USA, 2009.
37. Wu, S.; Yang, H.; Huang, S.; Chen, Q., Relationship between Reaction Kinetics and Chain Dynamics of Vitrimers Based on Dioxaborolane Metathesis. *Macromolecules* **2020**, *53*, 1180-1190.
38. Elling, B. R.; Dichtel, W. R., Reprocessable Cross-Linked Polymer Networks: Are Associative Exchange Mechanisms Desirable? *ACS Cent. Sci.* **2020**, *6*, 1488-1496.

39. Fortman, D. J.; Snyder, R. L.; Sheppard, D. T.; Dichtel, W. R., Rapidly Reprocessable Cross-Linked Polyhydroxyurethanes Based on Disulfide Exchange. *ACS Macro Lett.* **2018**, *7*, 1226-1231.
40. Breuillac, A.; Kassalias, A.; Nicolaÿ, R., Polybutadiene Vitrimers Based on Dioxaborolane Chemistry and Dual Networks with Static and Dynamic Cross-links. *Macromolecules* **2019**, *52*, 7102-7113.
41. Taplan, C.; Guerre, M.; Winne, J. M.; Du Prez, F. E., Fast processing of highly crosslinked, low-viscosity vitrimers. *Mater. Horiz.* **2020**, *7*, 104-110.

**TOC:**

